DRY-TO-WET TRANSITIONAL AVALANCHES: INFERENCES MADE USING INFRASOUND SURVEILLANCE

Jeffrey Johnson[1]*, Scott Havens[2], Timothy Glassett[3], Chris Stinson[3], Steven Clark[4], Jerry Mock[1,2], Hans Peter Marshall[1], Leighton Watson[5]

[1] Boise State University, Idaho, USA; [2] Snowbound Solutions, Idaho, USA; [3] Alaska Department of Transportation, Alaska, USA; [4] Utah Department of Transportation, Utah, USA; [5] University of Canterbury, Christchurch, New Zealand

ABSTRACT: The maritime climate of Turnagain Arm, near Anchorage, Alaska, provides snow conditions conducive to the generation of frequent large avalanches, which begin as dry powdery slab releases from as high as 1200 meters above sea level and transition to a wet avalanche, or slurry, by the time they reach sea level. This study identifies and characterizes the infrasound and low-frequency acoustic signatures (below 50 Hz) associated with these rapid gravity-driven snow mass movements by examining a sequence of eight avalanches triggered by howitzer artillery during an Alaska Department of Transportation hazard mitigation campaign on January 30th, 2026. Using coincident video, we quantify these mass movements in terms of their infrasonic source intensities, signal durations, and infrasound-inferred descent velocities and use the infrasound signal morphology to characterize the dynamics of these avalanches. Specifically, we are able to differentiate wet versus dry flow signal characteristics and energetics (which are higher frequency and lower intensity for wet debris). We also use the infrasound avalanche dataset to document multiple flow pulses (within an individual avalanche) and discuss isolated discrete infrasonic pulses possibly associated with flow accelerations or decelerations.

KEYWORDS: avalanche monitoring, infrasound, transitional avalanches

1. INTRODUCTION

Turnagain Arm is a waterway extending from Cook Inlet southeast from Anchorage, Alaska. The north shore of the Turnagain Arm accommodates a narrow transportation corridor including the Seward Highway and a freight rail line that is exposed to avalanche hazards from more than 50 recognized slide paths. This highway provides the only road access to a very large geographic area encompassing southcentral Alaska and it parallels both power lines and a buried gas pipeline, which are all in the avalanche runout zone and within 100 meters of each other.

Avalanche hazards are particularly high in this region due to heavy maritime precipitation, and frequent high winds depositing snow into the starting zones, as well as due to the steep topography extending from ~1200 m peaks down to sea level in about 2 km (giving rise to average slopes exceeding 37 degrees). A team from the Alaska Department of Transportation (AKDOT) is tasked with mitigating avalanche hazards to this critical transportation and resources corridor using howitzer cannons to trigger avalanches. During periods of high avalanche hazard, shells are fired from locations near sea level and aimed at target starting zones below a summit ridgeline as far as four kilometers away. Shells detonate upon impact with the ground or snowpack and generate pressure waves that load weak layers. This in turn can induce crack propagation and slab avalanche initiation in the dry, cold snowpack in the starting zones.

* Corresponding author address:
Jeffrey B Johnson, Boise State University;
tel: +1 208 971 5832
email: jeffreybjohnson@boisestate.edu

2. DEPLOYMENT GEOMETRY

On January 30, 2026 AKDOT performed a morning campaign to trigger avalanches along a stretch of the Seward Highway about 50 km from Anchorage in the vicinity of Bird Point (Figure 1). During an approximate 40-minute period from 9:23 AM to 10:04 AM the AKDOT team fired fourteen 105-mm shells from the 96.5 howitzer platform inducing eight avalanches that were well detected by a network of infrasound sensors. These infrasound sensors, installed and maintained by Snowbound Solutions LLC, were configured in a network of 3-element arrays deployed adjacent to the highway with network name Bird Flat (BF). Although array BF1 was not yet fully installed and operational, two of the three arrays (BF2 and BF3, which were separated by ~900 meters) recorded avalanches permitting triangulation of the moving sources using multi-array cross-beam processing as described in Marchetti & Johnson (2023). Generally, the avalanche acoustic signals recorded at BF2 and BF3 were evident starting about 25 to 30 seconds after the shot and within about ten seconds of the howitzer

https://doi.org/10.15788/1790098758

detonations. These 30 seconds of lag account for time-of-flight of the artillery (~10 s), time of acoustic propagation from high on the mountain (~10 s) and time for the avalanche to build in energy sufficiently to start producing infrasound.



Figure 1 – A perspective view from Google Earth showing the City of Anchorage (upper left), the Seward Highway, and the Bird Flat Launch Pad howitzer site. The black outlines correspond to the named slide paths detailed in Figure 2a.

The location of the infrasound arrays BF2 and BF3 were selected to optimize detection and localization of both triggered and natural snow avalanches occurring along a two kilometer section of Seward Highway (Figure 2a). An additional site BF1, to the west of BF2, became operational a few days later after installation was completed, but data were not yet available for the January 30th campaign. In general, the topology of the infrasound arrays informs the precision of acoustic source locations. Potential sources occurring within the region between these two arrays, considered *in-network*, are located with smaller uncertainties. Sources occurring *outside the* network have uncertainties that can be large and asymmetric as indicated by the ellipses in Figure 2b.

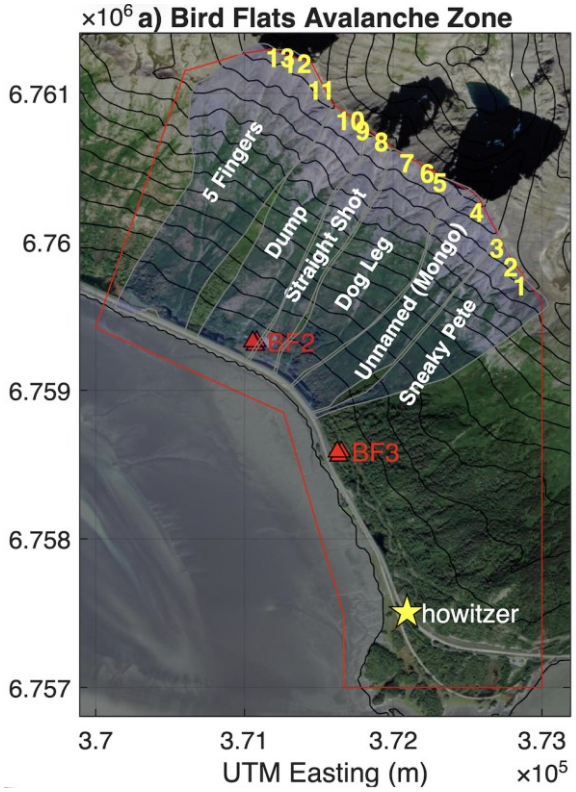


Figure 2a – Detail map of infrasound arrays (red triangles) and howitzer pad at sea level (yellow star) along with AKDOT detonation locations (indicated with numbers) for the morning of January 30, 2026. Names of slide paths and their outlines are shown. Contours in this map and other figures are drawn at 50-m intervals.

3. HOWITZER SHOTS/DETONATIONS

Both the launch infrasound and the detonation signals have energy extending from above 7 Hz up into the low frequency audible band (Figure 3). In general, the detonation infrasound, occurring high up near the ridgeline has variable signal morphology and amplitude shot-to-shot. Although all 105-mm howitzer shells deliver the same explosive yield, the difference in acoustic amplitudes is likely attributable to whether the explosion is a virtual airburst, occurring against rock or in shallow snowpack, or whether the detonation occurs in a thick snowpack. Additionally, there may be path effects, due to atmospheric winds and/or topography, that can impact recorded acoustic intensity due to airwave refraction and diffraction.

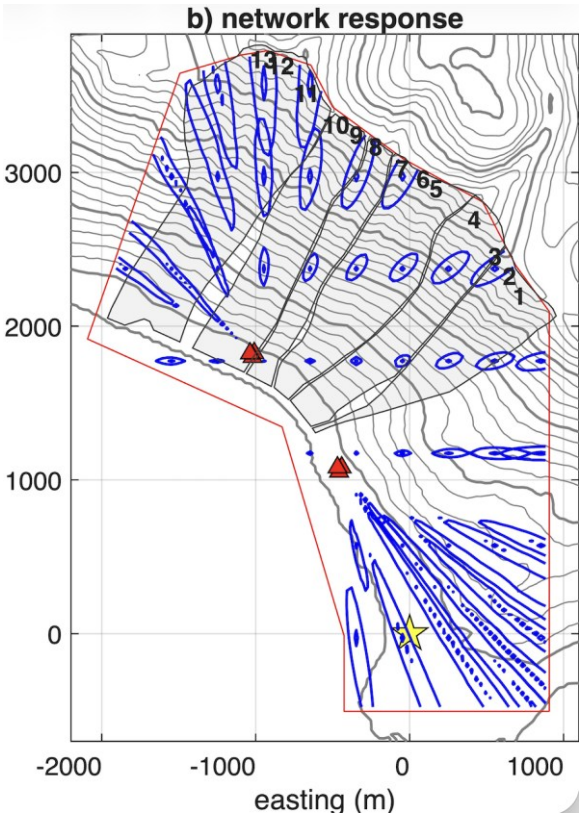


Figure 2b – Network response shows the precision of located infrasound sources given the array topology, which includes two three element arrays at BF2 and BF3. Elongate ellipses indicate location uncertainties. Northing and easting axes are referenced to howitzer pad location.

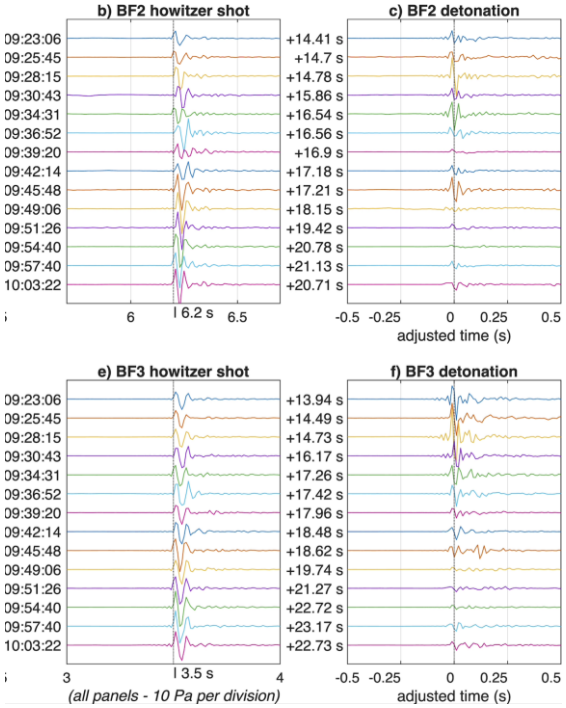
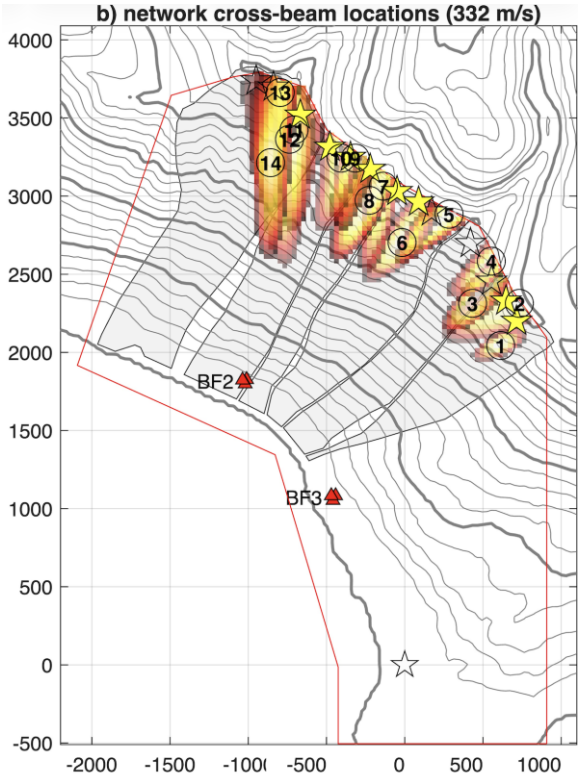


Figure 3 – Acoustic waveforms for Howitzer firing (shots) from near sea level (left panels) and detonations from elevation (right panels). Timing of shots from howitzer pad is indicated to the left of panels b and e. Detonation times, relative to local times is indicated in text left of panels c,f.

Howitzer detonations may be triangulated using arrival time information from all six channels on the two arrays. Differential travel times measured on a single array permit beamforming that can be used to point to the source of incident infrasound. Beamforming from two arrays can be used to find the location of a source in two dimensions. In the case of howitzer detonations, our algorithm calculates the semblance of each candidate source occurring within a search domain. The product of semblance from two arrays is plotted as a score and its contours are indicated in the polygons of Figure 4.

Figure 4 – (at right) Located howitzer detonations using semblance analysis and array processing with triangulation from two station. Yellow stars indicate target locations provided by AKDOT whereas circles with numbered shots correspond to infrasound localization using a homogenous sound speed of 332 m/s. Sources have been confined to the geographic domain outlined by the red polygon.



.

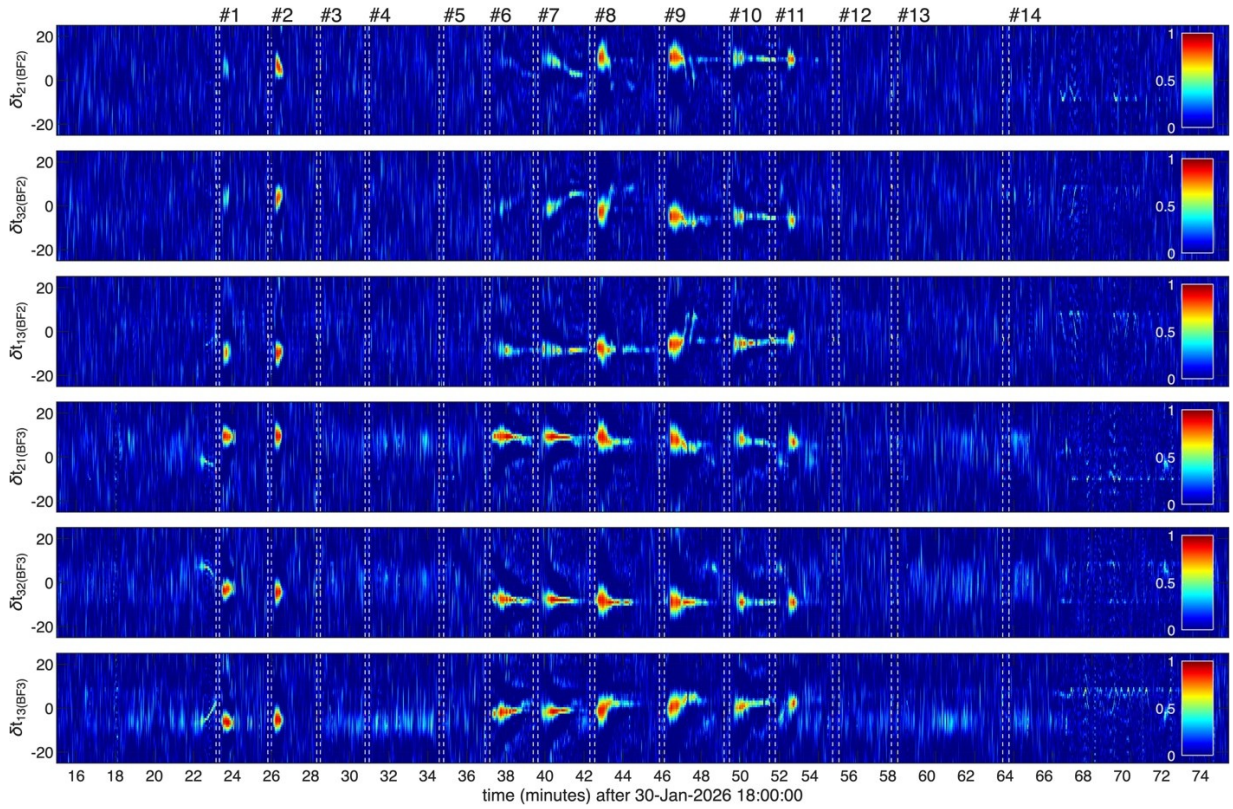


Figure 5 – Cross-correlation analysis ('correlograms') between six channels of infrasound at the two arrays during one hour. Top panel, for example, is a comparison between channel 2 and channel 1 at array BF2. Hot colors indicate signal correlation across these channels along with lag times (in samples) on the y-axis. Both howitzer firing times and detonation times are indicated as vertical white dashed lines.

4. AVALANCHE DETECTION + LOCATION

Unlike howitzer infrasound, which is generally short-duration and high-amplitude, snow avalanche acoustic signals are typically emergent, lower-amplitude, and sometimes obscured by noise. Array processing is thus essential for identifying signal that might otherwise be obscured by noise. The correlation analysis in Figure 5, for example shows clearly that there are 8 avalanches, several which have signals lasting for more than one minute, i.e., #6-10. These correlation lag times may be transformed into backazimuth chronologies (Figure 6) that hint at changing source positions as an avalanche sweeps downslope. The product of semblance at two arrays (Figure 6c) indicates an acoustic source that is well recorded across the network and is locatable (Figure 7). Different infrasound filter bands tested for greatest coherence suggest using the 1.5-40 Hz band is appropriate for avalanche signal at this site.

Avalanches were triggered for 8 of the 14 detonations and their cross-beam locations over time are indicated in Figure 7. Notably, events #1,2,6,7,8 are well triangulated, but event #9 on the Dump Slide Path descends *outside* the network north and west of both BF2 and BF3 such that its precise location is not as trustworthy. There is very little positional constraint for this event (green circles for event #9) as it progresses below 250 meters elevation. Elaborating upon this, the two pulses seen in the backazimuth plots of Figure 6a for BF2 (occurring at ~09:47 and 09:48 local time) appear to sweep past that station from northwest to west. These correspond to two notable surges in the wet slurry of blocks.

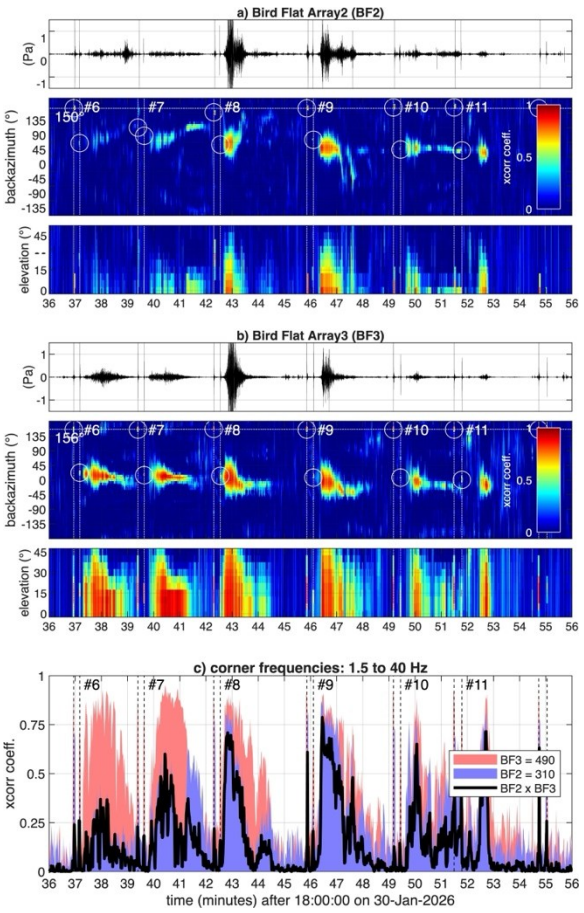


Figure 6 – Detail of shots #6-11 and corresponding infrasound waveforms along with backazimuth and elevation angles. Bottom panel (c) shows correlation scores over time (blue/rose color) along with their product (black line).

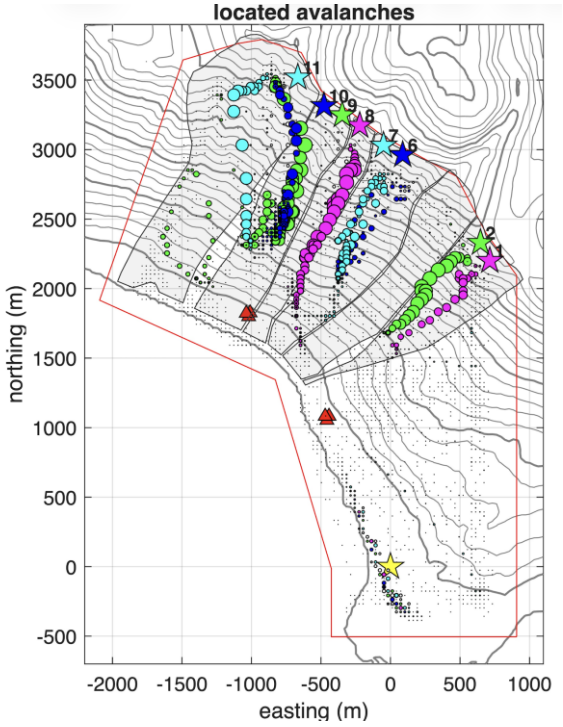


Figure 7 – Eight avalanches located using array cross-beam analysis for shots #1,2,6,7,8,9,10, and 11. Locations are calculated for 5-s windows at 1-s intervals with 4 seconds of overlap. Colors are used to distinguish the different events and correspond to the AKDOT howitzer detonation locations (stars). For instance, the green circles in the upper left correspond to the shot #9. Size of circle symbols corresponds to normalized cross-correlation scores.

5. DISCUSSION

From video observations taken coincidentally with infrasound recordings it is possible to observe that all of the featured avalanches begin with howitzer detonations and initially exhibit acoustic features of a standard powder cloud avalanche [e.g., Johnson et al., 2021a], corresponding to fast-moving dry snow, a voluminous powder cloud, and a turbulent air flow. Correlation between video and acoustic signal suggests that these dry clouds are coincident with the generation of the highest amplitude acoustic signals and in the case of the events featured here last up to 40 seconds. However, that is only the first part of the acoustic signal for events #6-10. Following this initial phase there is continuing signal detectable for many of the events lasting another minute.

This acoustic coda - despite its location closer to the infrasound arrays - is smaller in amplitude and tends to appear stationary in terms of its back azimuth. It also corresponds to a relatively higher frequency acoustic range extending well above 10 Hz (Figure 8). These higher frequencies coincide with the later stage of the flow, when a wet avalanche slurry is adjacent to the monitoring sites. At that point the arrays likely pick up on the most proximal source of flow acoustic signal and point in that direction consistently until the flow has diminished. One good exception is event #9 where two moving pulses can be detected at around 09:47:10 and 09:47:30 (Figure 6a) when two surges are clearly evident as moving sources on BF2.

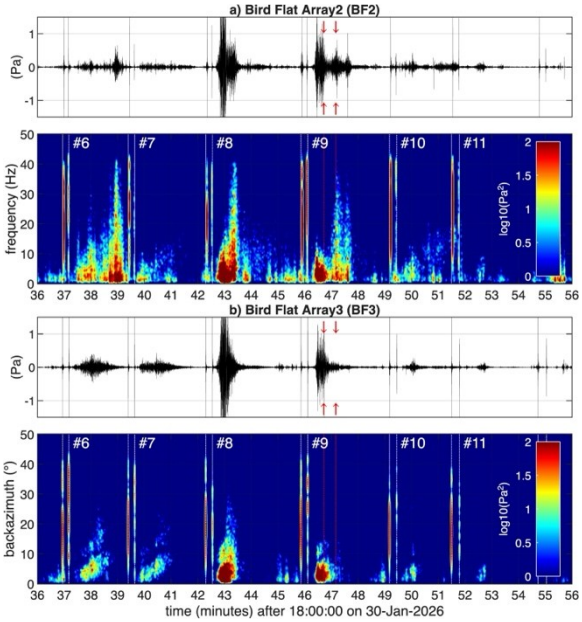


Figure 8 – Waveforms and spectrograms for six of the eight avalanches recorded on both arrays. Red arrows show timing of the images in Figure 9a,b grabbed from video grabbed from video.

6. CONCLUSIONS

At distances less than a few kilometers avalanche infrasound source locations can often be effectively mapped [e.g., Watson et al., 2022] and an avalanche's descending progress can be tracked using single sensor arrays [e.g., Havens et al., 2014; Ulivieri et al., 2011] as well as a network of two or more infrasound arrays [e.g., Johnson et al., 2021]. The two-array approach that is applied here integrates array beamforming at individual arrays and triangulation of moving sources as they flow downslope.



Figure 9a – View of triggered avalanche powder cloud descending Dump at 09:46:43 corresponding to first red arrows in Figure 8. Camera was located just west of the BF2 array.



Figure 9b – 1 View of snow slurry and blocky flow near bottom of Dump Slide Path at 09:47:10 corresponding to second red arrows in Figure 8.

In the case of the dataset of 8 avalanches from 30-Jan-2026, at least 5 exhibited relatively long-duration acoustic signals lasting as long as two minutes. This coda, occurring after about 45 seconds, coincides with observations of slurries of wet snow blocks moving adjacent to the infrasound stations. We have shown that the infrasound signal from these wet slurries produces locatable sound of generally higher frequencies and diminished amplitudes. Given their high frequencies and lower amplitudes we conclude that their acoustic detection would be difficult at distances greater than about one kilometer. We suspect that these dense flows of wet snow and blocks would be amenable to seismic detection, a current focus of ongoing research.

ACKNOWLEDGEMENTS

This work was partially supported through the research program of the Transportation Avalanche Research Pool (TARP) through the CDOT Research Office study No. 497-24-07. Boise State University researchers Jacob Anderson and Owen Walsh contributed to the development of the infrasound sensors used in this work.

We remember Liz Clabaugh and eight others who died in a snow avalanche in California on February 17th, 2026. Liz was friend and family to the authors of this paper. This research is dedicated to her.

REFERENCES

Havens, S., Marshall, H.-P., Johnson, J. B., & Nicholson, B. (2014). Calculating the velocity of a fast-moving snow avalanche using an infrasound array. *Geophysical Research Letters*, *41*(17), 6191–6198. https://doi.org/10.1002/2014GL061254

Johnson, J. B., Anderson, J. F., Marshall, H. P., Havens, S., & Watson, L. M. (2021). Snow Avalanche Detection and Source Constraints Made Using a Networked Array of Infrasound Sensors. *Journal of Geophysical Research: Earth Surface*, *126*(3), 1–23. https://doi.org/10.1029/2020JF005741

Johnson, J. B., Marshall, H. P., & Anderson, J. F. (2021). *Infrasound avalanche monitoring: Enhanced monitoring in Little Cottonwood Canyon, Utah*. Retrieved from https://rosap.ntl.bts.gov/view/dot/60194

Marchetti, E., & Johnson, J. B. (2023). *Infrasound array analysis of rapid mass movements in mountain regions*. (C. Schmelzbach, Ed.), *Advances in Geophysics: Geohazards* (Advances i, Vol. 64). Zurich: Academic Press.

Ulivieri, G., Marchetti, E., Ripepe, M., Chiambretti, I., De Rosa, G., & Segor, V. (2011). Monitoring snow avalanches in Northwestern Italian Alps using an infrasound array. *Cold Regions Science and Technology*, *69*(2–3), 177–183. https://doi.org/10.1016/j.coldregions.2011.09.006

Watson, L. M., Carpenter, B., Thompson, K., & Johnson, J. B. (2022). Using local infrasound arrays to detect plunging snow avalanches along the Milford Road, New Zealand (Aotearoa). *Natural Hazards*, *111*(1), 949–972. https://doi.org/10.1007/s11069-021-05086-w